Chapter 2 Krib-Mejez el Bab Area

2.1 Geological Background

2.1.1 Regional Geology of the Republic of Tunisia

(1) Geology and Geological Structure

The geology of Tunisia can be structurally divided into the northern and southern geologic provinces in principle. The northern geologic province, situated in the east end of Atlas Range extending from northern Morocco through northern Algeria, belongs to the Alpine Orogenic Belt and consists of Mesozoic and Cenozoic groups. The southern geologic province is situated in the northern end of Sahara and consists of Palaeozoic, Mesozoic and Cenozoic groups.

Terrestrial sedimentary rocks of Tertiary extensively distribute in the southern province, forming aeolian sand-dunes in the desert of Sahara, and largely cover the Palaeozoic and Mesozoic groups with limited exposures. The Palaeozoic group comprises terrestrial or neritic sediments in the Saharan platform, while the Mesozoic group consists of sedimentary rocks equivalent to that in the northern province as described below.

Mesozoic and Cenozoic groups, consisting mainly of sedimentary rocks, extensively distribute in the northern province and form a stratigraphic sequence without major hiatus. Since their distribution is largely controlled by the NE-SW trending structures, the geologic province is subdivided into five structural zones from northwest to southeast, namely, the Nappe, the Dome, the Trough, the N-S Axial and the Eastern Platform zones (Orgeval, 1994). The geologic map and the map of the structural zones of the northern part of the Republic of Tunisia are shown in Figure 3 and 4 respectively.

The Mesozoic group in the northern geologic province comprises Triassic (dolomite, marl, argillite, sandstone, limestone, clay, gypsum and rock salt), Jurassic (limestone, dolomite, marl, argillite and sandstone) and Cretaceous (limestone, marl, argillite, sandstone and dolomite) systems. The Cretaceous system widely distributes in the entire geologic province, while the Triassic system forms a number of blocks of variable sizes. Distribution of the Jurassic system is very much localized. Igneous rocks are extremely rare in their occurrences, which include granite forming Galite Island, the northernmost landform in the territory of the Republic of Tunisia, and very minor Neogene basalt distributing in the Nappe zone.

The Triassic system occurs mainly in the Dome zone, forming discontinuous domes or evaporite diapirs elongating and arranged in the NE-SW direction. The Jurassic system is sporadically exposed in 'small windows' in the N-S axial zone trending in the N-S

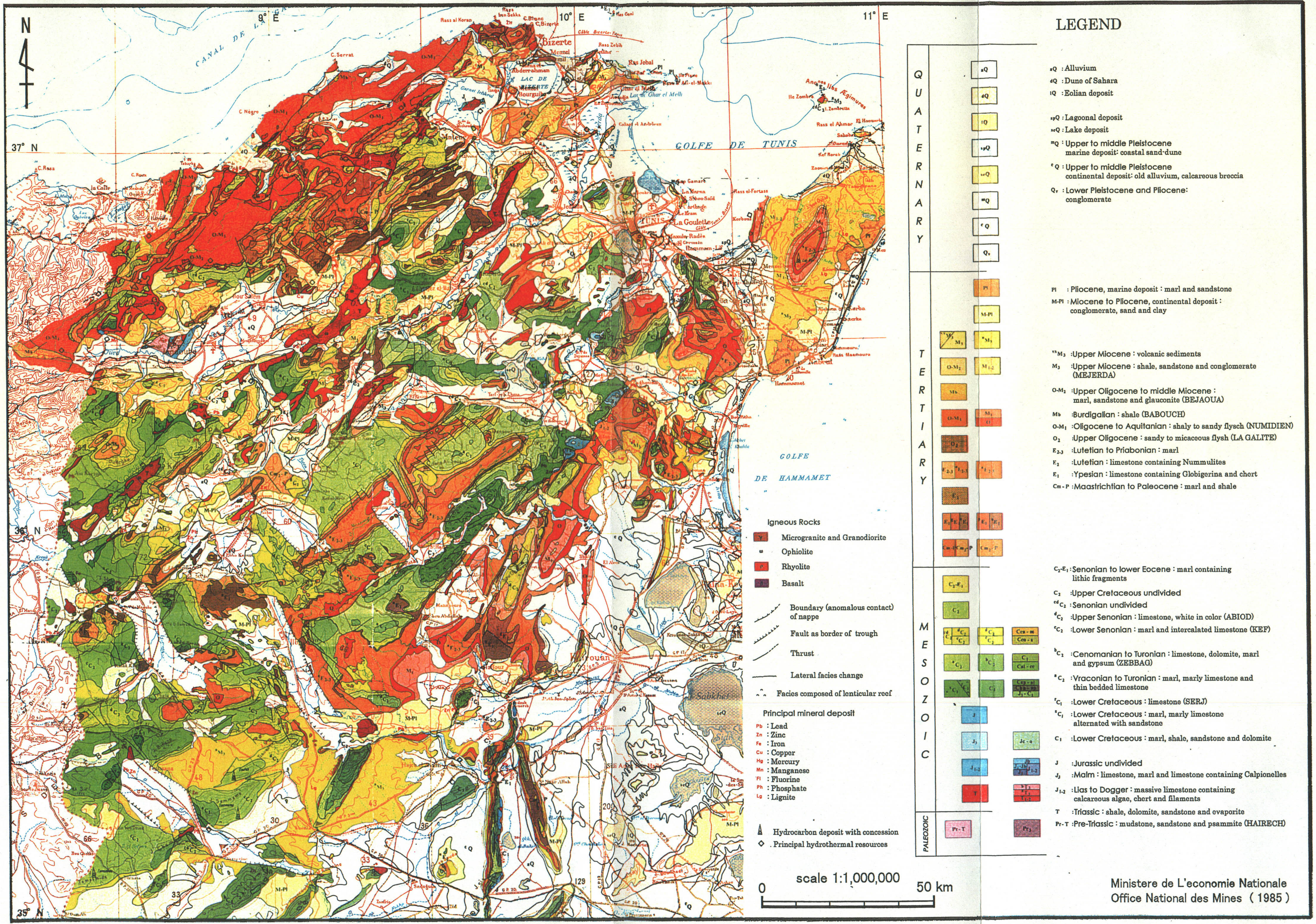

Figure 3 Geologic map of northern Tunisia

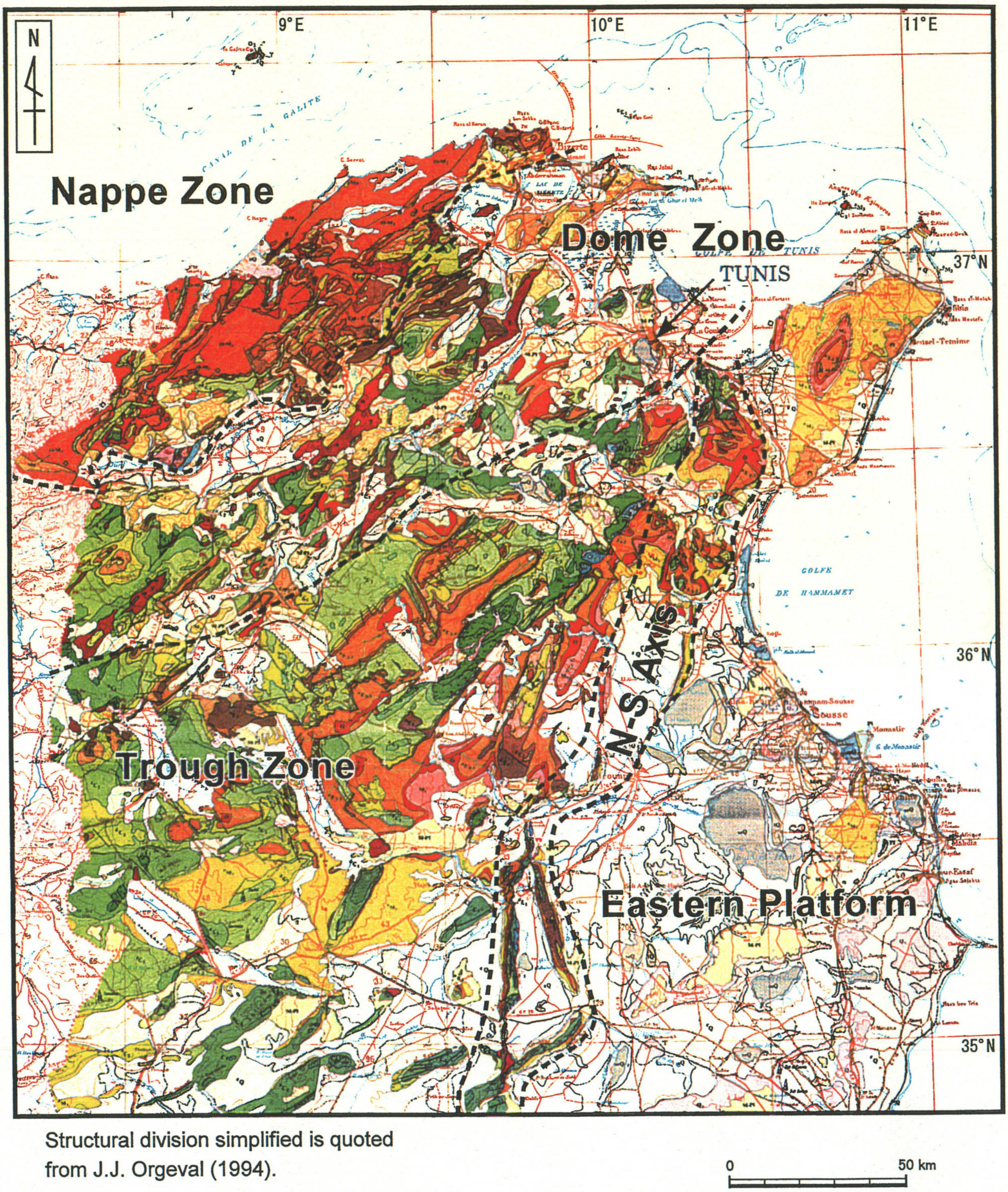

Structural division simplified is quoted from J.J. Orgeval (1994).

Geological base map is published in 1985 by Ministere de L'economie Nationale. (Legend of the map is shown in Figure 2)

Figure 4 Structural zones of northern Tunisia direction, but rarely distributes in the Dome zone. Distribution of the Cretaceous system is particularly extensive in the Dome and Trough zones. Its sedimentary structures are often deformed by intrusion of diapirs of the Triassic system. However, its strata generally strike in the NE-SW direction that corresponds to the distribution trend of the Triassic system. Major thrust faults and folding axes also trend in the NE-SW direction, while most strike-slip faults and associated fracture systems indicate the NW-SE direction.

The Cenozoic group comprises sedimentary rocks of the Tertiary and Quaternary system systems. The Tertiary system is further subdivided into Palaeogene (Palaeocene, Eocene and Oligocene series) and Neogene (Miocene and Pliocene series) subsystems. The Tertiary system consists mainly of flysh sediments (marl, argillite, limestone and sandstone) in the Nappe zone in the north, and mainly of limestone, argillite, marine and terrestrial sandstone, and marl in the Dome and Trough zones. The geological structure of the Nappe zone is extremely complicated by considerable development of a number of thrust faults and overturned folds. The sedimentary structure of the Dome zone is also highly disturbed due to intrusion of diapirs of the Triassic system. The principal structure of the Tertiary system in the Dome zone is represented by the fracture systems trending in the NE-SW and the NW-SE directions as is the case for the Cretaceous system. The Quaternary system consists of gravel, terrestrial sandstone and aeolian, colluvial and alluvial deposits.

A majority of metalliferous deposits in Tunisia are those of lead-zinc, followed by copper, iron and mercury deposits as well as non-metallic deposits such as phosphate and fluorite. A number of Pb-Zn deposits are located mainly in the Dome zone in northern Tunisia. They occur spatially in close association with diapirs of the Triassic system at or in the proximity to their contacts with the Cretaceous and Tertiary systems, and are categorized into the Mississippi Valley type. Cu and Hg deposits are genetically related to granitic rocks mainly distributing in the Nappe zone. Phosphate deposits are of a sedimentary type formed in marine sediments of Cretaceous to Eocene and mainly distribute in central Tunisia.

(2) Geologic History

A platform sedimentary basin was formed in a vast area of the present northern margin of African Shield during the period of the latest Precambrian to early Palaeozoic. The sediments that deposited in the basin in the periods of Cambrian to Ordovician and of Carboniferous comprise marine sequences in the present location of Algeria and alternation of marine and terrestrial sequences in that of Libya. These platform sediments, showing nearly flat attitudes, have been least affected by Variscan (Hercynian) Orogeny of late Palaeozoic. This region of northern Africa, including Tunisia, was placed under a neritic sedimentary environment during Triassic. This neritic sedimentary basin intermittently emerged above sea surface during Triassic, which resulted in deposition of neritic sediments including evaporite components such as gypsum, rock salt and dolomite.

Towards Jurassic, the Super Continent, Pangea, was broken into Eurasian in the north and Gondwana in the south, with development of Tethys Sea in between. As Tethys Sea transgressed, the sedimentary basin of this region along the northern margin of Gondwana was separated into the northern trough (Tunisian trough) and the southern neritic shelf. Thick sequences of upper Jurassic to Cretaceous sedimentary rocks of deep-water facies were deposited in the Tunisian trough, with the estimated thickness of some 5000m for the Cretaceous system alone. On the other hand, the stratigraphic equivalents in the southern neritic shelf were much less in their thickness and characterized by reef facies.

Prior to middle Cretaceous, relative movement of structural blocks prevailed in the region and initiated diapirism in late Aptian. As the Alpine diastrophism emerged in late Cretaceous, the sedimentary basin became progressively shallower towards early Tertiary and more and more continental in nature. The Tunisian trough no longer existed as a palaeogeographic unit by middle Eocene.

The Alpine diastrophism, with its peak stage in Oligocene, brought about intense deformation of rocks in the region by folding, faulting and thrusting during the period of Neogene. These structures were formed under the prevailing stress field in the period, indicating mostly the principal trend of NE-SW direction. Particularly, a number of nappes were tectonically brought into the region from north to form the 'Nappe zone'. The entire region continued uplifting towards Pliocene or later and was elevated to the present level of Atlas Range.

Most of diapirs, comprising Triassic evaporites and other neritic sediments, were halocinetically introduced in the period of late Cretaceous and were reformed and rearranged in the course of the tectonic development as above explained. A number of Pb-Zn ore deposits, together with other associated minerals, were formed in close association, spatially or genetically, with diapirs in various stages of sedimentary and tectonic processes.

2.1.2 General Geology of the Krib-Mejez el Bab Area

The Krib- Mejez el Bab Area is situated within the Dome zone, to the southwest of Tunis. The Dome zone is about 50 km wide and some 200 km long in the NE-SW direction, bounded by the Mediterranean Coast to the northwest, and continues southwestward across the international border to Algeria (Figure 4). A number of Triassic diapirs are discontinuously aligned in the NE-SW direction within the Dome zone, forming 3 or 4 major diapir alignments. The Project Area is located in the middle part of the southeastern-most alignment.

The geology of this Area comprises Triassic, Cretaceous, Palaeogene, Neogene and Quaternary systems in stratigraphically ascending order. The Triassic system forms diapirs which have intrusive contacts with the Cretaceous, Palaeogene and Neogene systems or partly overlie these systems. The geology is shown in Figure 5.

The Triassic system, comprising gypsum, clay, dolomite, argillite, sandstone and limestone, is generally inhomogeneous in its facies and often indicates disturbed sedimentary structures. No Jurassic system crops out in the Area. The Cretaceous system consists of stratigraphycally continuous successions of Barremian through Maastrichtian comprising limestone, marl, argillite, sandstone and dolomite. Beddings of these sedimentary rocks strike generally in the NE-SW direction, however, are often disturbed near contacts to diapirs or along faults. The Tertiary system also consists of stratigraphically continuous successions of Palaeocene, Eocene, Oligocene, Miocene and Pliocene series. The Palaeocene series is composed of argillite, the Eocene, of conglomerate and limestone, and the Oligocene, the Miocene and the Pliocene, of sandstone. The general strikes of beddings run in the NE-SW direction, however, vary near contacts to diapirs or according to structures of sedimentary basins. Strata of the Cretaceous and Tertiary systems are extremely turned over in the vicinity of diapir bodies, indicating vertical or reversed attitudes. The Quaternary system comprises sandstone, conglomerate, alluvial deposits, talus deposits and so forth.

There are three sizable diapir bodies in the Project Area and called Mourrha, Jebel ech Cheid and Bou Khil respectively from northeast to southwest. Several smaller diapir bodies are also known around these major diapirs and are mostly elongated in the NE-SW direction. A number of Pb-Zn ore deposits or mineral occurrences are located in association with these diapirs. They indicate specific spatial relationship with the diapirs, being mostly positioned at either edge of elongated diapirs or along their southeastern flanks. The modes of occurrences of the three major diapirs are summarized below.

- Mourrha: This diapir shows a 5x3 km rectangular form with rounded corners on plan and a mushroom shape on cross section. Its southeastern flank contacts mainly with the Cretaceous system and partly with Eocene or Oligocene series. Other parts of its outer limit are covered by the Quaternary system. Kef Lasfer and Oued Jebes ore deposits are located along the southeastern flank.
- Jebel ech Cheid: This diapir is 23 km long and 5 km wide, and by far the largest of all in the general area. It takes a bamboo leaf form on plan and a mushroom shape on cross section. Its northeastern half contacts with the Eocene, Oligocene or Miocene series, while the southwestern half mostly contacts with the Cretaceous system. A roof-pendant of the Oligocene and Miocene series covers the top of the

diapir body in its center. There are known a number of ore deposits and mineral occurrences along the southeastern flank of the diapir, such as Koudiat Tlilett, Koudiat Soda, H'Zamel Assoued, Koudiat Bazina Kebira and Argoub Adama. El Akhouat deposit is located in the vicinity of the diapir body, to the southwest of its southwestern edge.

- Bou Khil: This diapir body forms a crescent shape, 7 km long and 3 km wide. Its southeastern flank contacts with the Cretaceous system, Oligocene series or Pliocene series, while the northwestern flank is covered by the Cretaceous system. There is located Bou Khil deposit in the central southeast of the diapir body and Jebel Ouiba mineral occurrence at its northeastern edge.

In addition, Fedj el Adoum Mine, one of the two Pb-Zn mines being currently operated in Tunisia, is located about 10 km northwest of Bou Khil diapir, outside of the Project Area, and is associated with Fedj el Adoum diapir.

Figure 5 is a cross section showing a schematic profile of Triassic diapirs across the Nappe through the Dome zones. Each diapir has its own size and shape, and varies in its period of diapirism. The following process is generally accepted for formation of diapirs in this region.

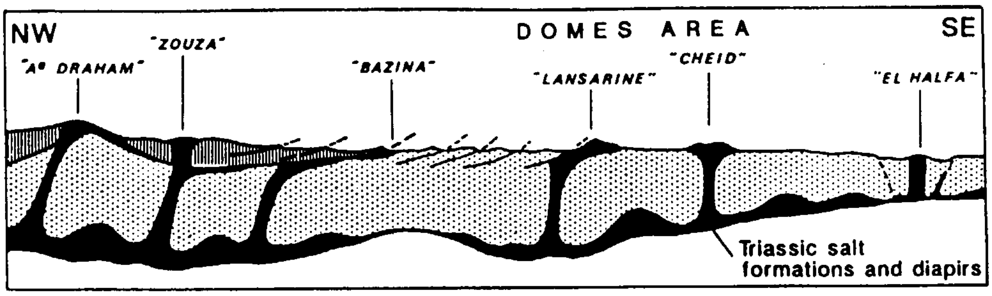

Simplified cross section, from the Nappe zone to central Tunisia, showing the distribution of Triassic structures and the progressive dying out of the tangential tectonics from northwest to southeast. The Domes area corresponds to the Lansarine and Cheid diapirs. (After Perthuisot 1978)

Figure 5 Schematic profile of Triassic diapers (J.J. Orgeval, 1994)

The diapirism, which initiated in mid-Cretaceous in this region, was upheaval of the Triassic system, containing evaporite components, into the overlying Cretaceous system mainly due to difference in density between the two systems. The upheaval in its early stage may have taken place in accordance with the morphology of the sedimentary basins or the prevailing stress field in those days. Most diapirs were emplaced during the period of late Cretaceous, as aforementioned. As the diapirism proceeded, sedimentation of the late Cretaceous sequences became slower nearing diapir bodies and faster away from them. It is also reported that some of diapirs emerged out of the sea bottom through the overlying Cretaceous system at some stages of the diapirism. The Alpine diastrophism reached its climax in Oligocene and tectonically affected the entire region and therefore emplacement of diapirs. Simple original forms of diapirs, such as domes or mushrooms, were deformed and dislocated by faulting, thrusting and folding under the compressive stress field in the NW-SE direction before taking the present forms and positions.

The Pb-Zn mineralization is categorized into the 'Mississippi Valley' or 'Carbonate Hosted' type. It is interpreted that the mineralization is formed in the process that (1)intra-strata water dissolves Pb, Zn and other metals in sediments, (2) moves laterally along stratification, (3) ascends along diapirs and then (4) precipitates these metals in fractures, cavities or other open spaces within or in the vicinity of diapirs. Most Pb-Zn mineral occurrences are localized in the southeastern flanks of diapirs (in the right hand side in Figure 3). This implies that minor faults and fractures for sites of mineralization are well developed in the Cretaceous and Tertiary strata under diapir overhangs in the southeastern flanks due to over-folding. Another possibility may be that the southeastern flanks provide conduits favorable for ascending mineralized solutions and pressure and temperature conditions suitable for precipitation of metals.

2.2 Satellite Image Analysis

2.2.1 Objective and Area for Satellite Image Analysis

The objective of the satellite image analysis is to regionally interpret geological structure and lithology of the Project Area in order to provide background information for air photo interpretation and geological prospecting.

The area for image analysis is bounded by lines connecting the four corner points, of which coordination is indicated in Table 6, and occupies an area of approximately 550 km^2. Its location is illustrated in Figure 6.

Table 6 Area of Satellite Image Analysis

Corner	Longitude	Latitude
Upper Left	9° 40′ 10.3″ E	36° 39′ 05.0″ N
Upper Right	9° 43′ 02.6″ E	36° 36′ 13.9″ N
Lower Left	9° 03′ 10.4″ E	36° 16′ 03.4″ N
Lower Right	9° 10′ 24.6″ E	36° 10′ 44.6″ N

Table 9 LANDSAT-TM Map Projection Parameters

Coordination System	UTM
UTM Zone Center Longitude of Zone 32	32 9.00000° E
Projection	Transverse Mercator
Earth Model	WGS84
Sub-scene Coordination (UTM)	
Upper Left Lower Right	500,000.000E, 4,057,938.798N 575,277.425E, 3,984,270.969N

(3) False Color Image

① RGB=3·2·1 (Figure 7)

This image is produced by assigning three primary additive colors, red, green and blue to Bands 1, 2 and 3 respectively. This band combination presents colors of objects close to those sensed by human eyes. The image of the Project Area expresses vegetated lands in black or dark brown, bare grounds in white, light green or light brown, and cultivated lands in brown, light brown or light gray. Although topographic features and geological structures can be recognized on this image, lithological differentiation is very difficult.

② RGB=7·4·1 (Figure 8)

The combination of Band 7, 4 and 1, to which red, green and blue are respectively assigned, is designated for generating a false color image, which makes it possible to distinguish clay alteration zones, carbonate rocks and iron oxide zones. Band 7 will provide spectral features specific for clay minerals and carbonates, while iron oxides can be identified by combination of spectral features in Bands 1 and 4. This image is generated by adding Band 7 (2.08-2.35 μm) of SWIR region to the two bands (Bands 1 and 4) of VNIR region, and presents a variety of color features in comparison with the above two images (Figures 7) generated by three bands only of VNIR region. For example, hills on the image indicate variable colors, such as green, dark green, purple, yellow, light green, light gray and so forth, which may reflect differences in lithology. Topography, geological structures and land uses can be also recognized on the image.

(4) Principal-Component Image (Figure 9)

The main purpose of principal-component analysis is to compress a huge volume of complex multi-spectral data into three major groups of correlative data (principal components), in order to express a number of factors by three primary additive colors, namely, red, green and blue (RGB). Data of Band 1 through 5 and Band 7, excluding those of Band 6, are used for the principal-component analysis. The results are indicated in Table 10 and 11.

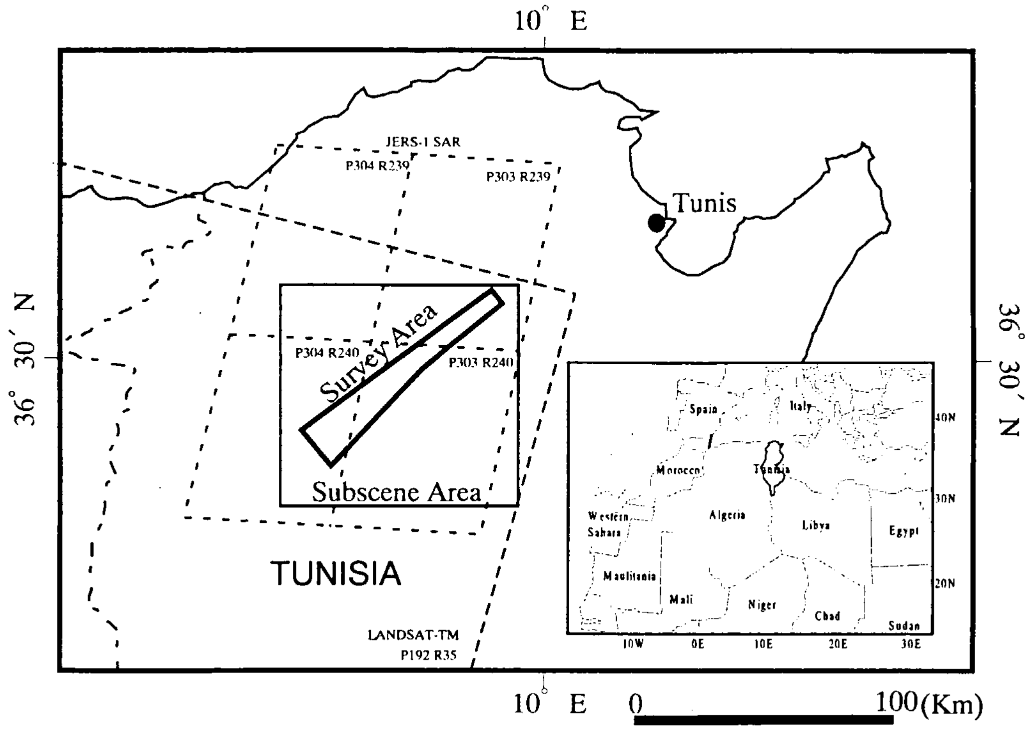

Figure 6 Satellite Image Location Map

2.2.2 LANDSAT-TM Image Analysis

(1) Data

Specifications of LANDSAT -TM data, which are used for the image analysis, are presented in Table 7. The data have been acquired in a month of the dry season (September), when vegetation activity is minimal in a year.

Table 7 LANDSAT-TM Data Specifications

Sensor	Path	Row	Date of Data Acquisition
LANDSAT-TM	192	35	Sep. 13, 1987

As shown Table 8, the LANDSAT -TM data comprises multi-spectral images of 4 bands in visible infrared region (bands 1 through 4), 2 bands in short wave infrared region (bands 5 and 7) and 1 band in thermal infrared region (band 6).

Since trivalent iron displays its absorption spectra in VIR region as aforementioned, the bands 1 through 4 are effective to detect iron oxides such as hematite, jarosite, goethite and limonite. In particular, reflectance of these minerals is invariably low in the band 1 wavelength range of 0.45-0.52 μ m in comparison with that of other minerals. The band 7 with the wavelength range of 2.08-2.35 is effective to detect clay minerals and carbonates inclusively, though differentiation of these minerals is conditional.

Table 8 LANDSAT-TM Observation Parameters

Band	Wavelength Range (μm)	Spatial Resolution (m)	Swath (km)
1	0.45-0.52	30	185
2	0.52-0.60	30	185
3	0.63-0.69	30	185
4	0.76-0.90	30	185
5	1.55-1.75	30	185
6	10.40-12.50	120	185
7	2.08-2.35	30	185

(2) Image Processing

A sub-scene comprising 2,685 pixels x 2,628 lines, which includes the area for image analysis, is framed out of a full scene of LANDSAT -TM image after the full scene data sets are georectified by using map projection parameters presented in Table 9. The sub-scene data sets are used for generating various false color and principal-component images.

Table 9 LANDSAT-TM Map Projection Parameters

Coordination System	UTM
UTM Zone	32
Center Longitude of Zone 32	9.00000° E
Projection	Transverse Mercator
Earth Model	WGS84
Sub-scene Coordination (UTM)	
Upper Left	500,000.000E, 4,057,938.798N
Lower Right	575,277.425E, 3,984,270.969N

(3) False Color Image

① RGB=3·2·1 (Figure 7)

This image is produced by assigning three primary additive colors, red, green and blue to Bands 1, 2 and 3 respectively. This band combination presents colors of objects close to those sensed by human eyes. The image of the Project Area expresses vegetated lands in black or dark brown, bare grounds in white, light green or light brown, and cultivated lands in brown, light brown or light gray. Although topographic features and geological structures can be recognized on this image, lithological differentiation is very difficult.

② RGB=7·4·1 (Figure 8)

The combination of Band 7, 4 and 1, to which red, green and blue are respectively assigned, is designated for generating a false color image, which makes it possible to distinguish clay alteration zones, carbonate rocks and iron oxide zones. Band 7 will provide spectral features specific for clay minerals and carbonates, while iron oxides can be identified by combination of spectral features in Bands 1 and 4. This image is

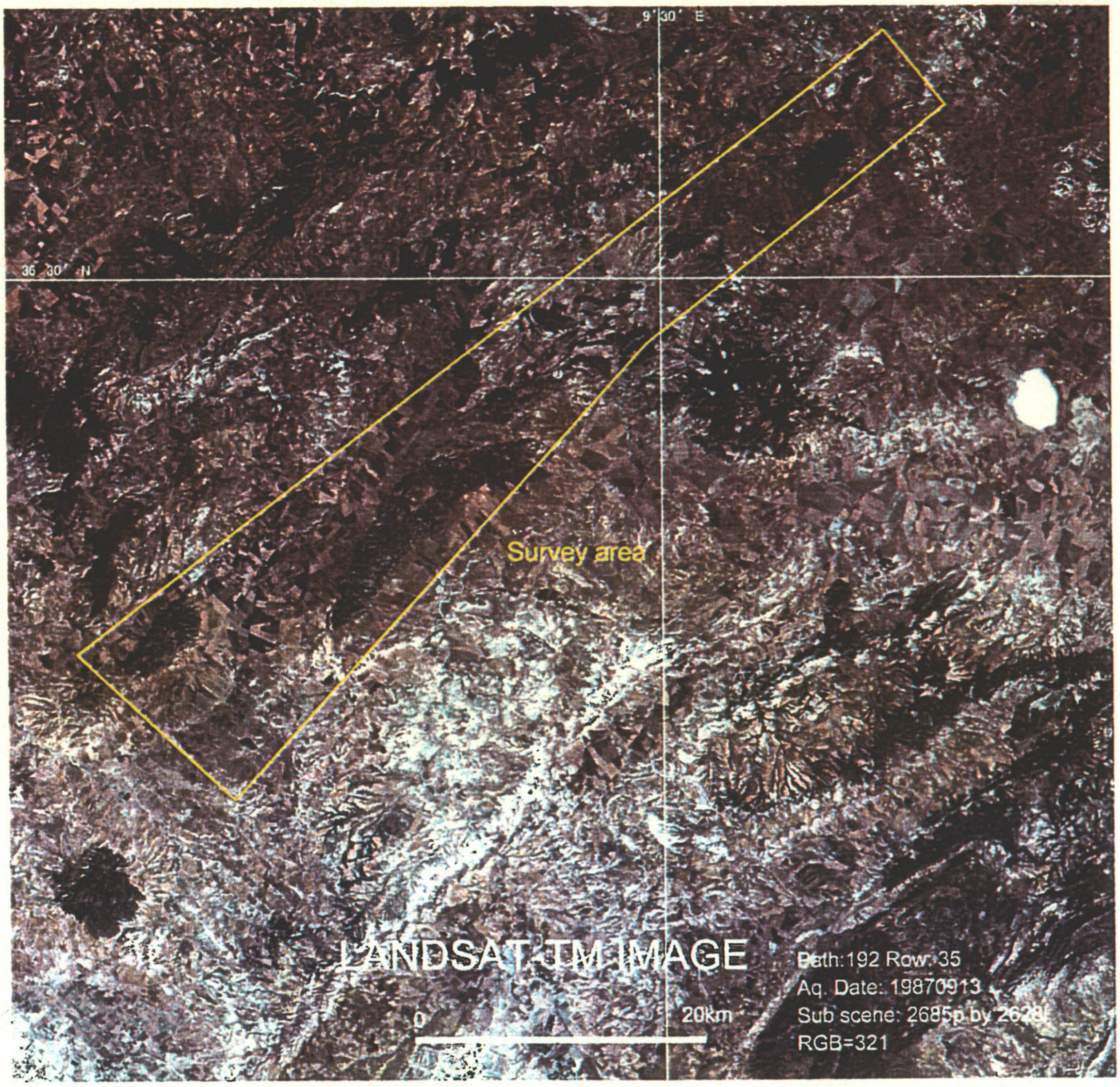

Figure 7　　False color composite image of Landsat-TM image (RGB=3・2・1)

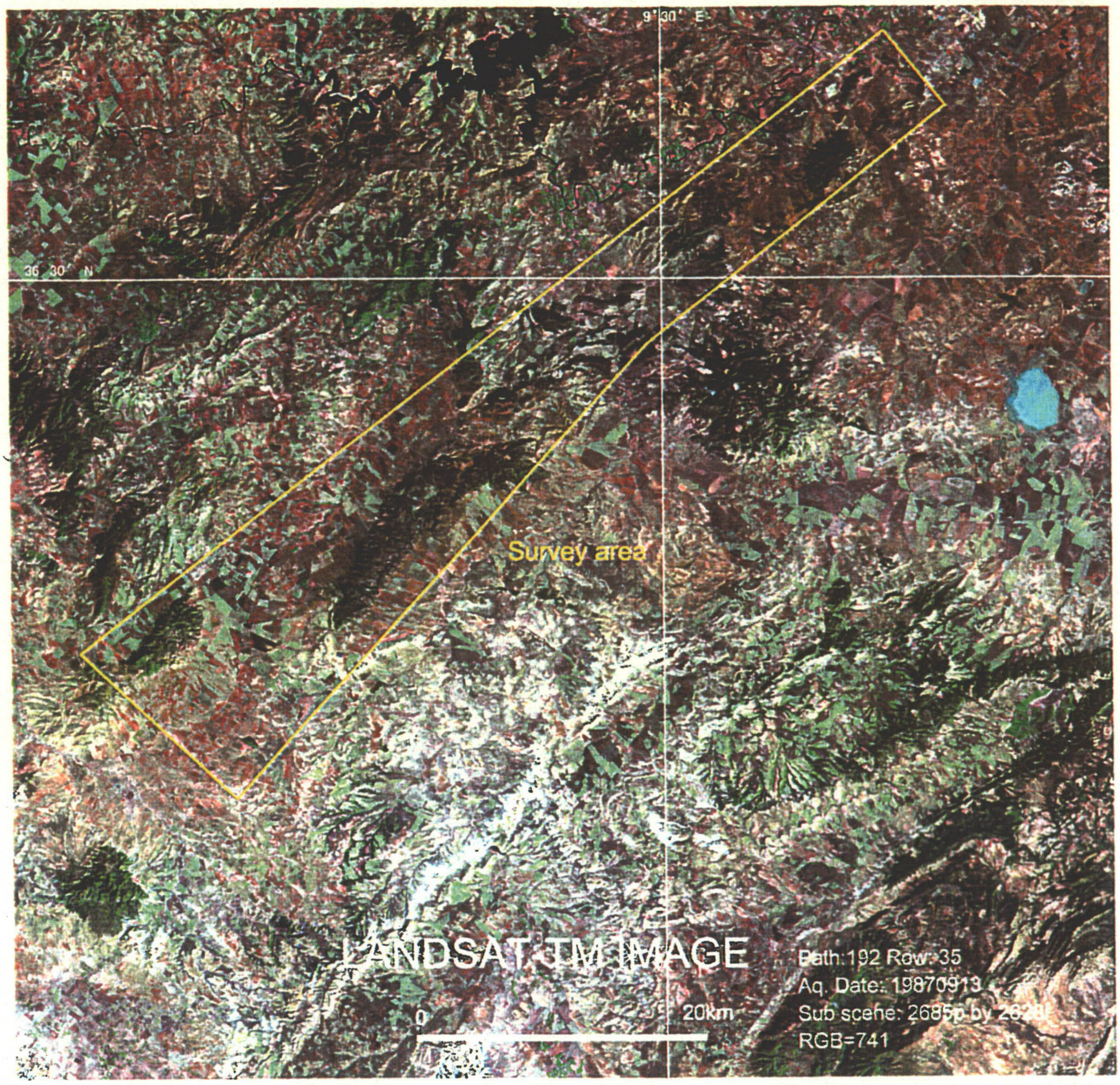

Figure 8 False color composite image of Landsat-TM image (RGB=7・4・1)

generated by adding Band 7 (2.08-2.35 μm) of SWIR region to the two bands (Bands 1 and 4) of VNIR region, and presents a variety of color features in comparison with the above two images (Figures 7) generated by three bands only of VNIR region. For example, hills on the image indicate variable colors, such as green, dark green, purple, yellow, light green, light gray and so forth, which may reflect differences in lithology. Topography, geological structures and land uses can be also recognized on the image.

(4) Principal-Component Image (Figure 9)

The main purpose of principal-component analysis is to compress a huge volume of complex multi-spectral data into three major groups of correlative data (principal components), in order to express a number of factors by three primary additive colors, namely, red, green and blue (RGB). Data of Band 1 through 5 and Band 7, excluding those of Band 6, are used for the principal-component analysis. The results are indicated in Table 10 and 11.

Table 10 Eigenvalues and Contributions of Principal Components

Eigenchannel	Eigenvalue	Deviation	Contribution
PC1	3308.2209	57.5171	90.84%
PC2	224.3998	14.98	6.16%
PC3	71.4512	8.4529	1.96%
PC4	22.8297	4.778	0.63%
PC5	12.4711	3.5314	0.34%

Table 11 Variance-Covariance Matrix of Eigenvector and Eigenvalue

	Band_1	Band_2	Band_3	Band_4	Band_5	Band_7
PC1	0.31187	0.23429	0.42717	0.3041	0.65672	0.37633
PC2	0.49195	0.33167	0.38159	0.29643	-0.51948	-0.38032
PC3	-0.40257	-0.18396	-0.06769	0.75454	0.20107	-0.43562
PC4	-0.14969	-0.00997	0.46023	-0.49694	0.36215	-0.62256
PC5	0.60781	-0.03198	-0.61225	-0.04084	0.34804	-0.36318

The 1st order principal component (PC-1) indicates high positive values in eigenvector for all 6 bands and is high in its contribution at 90.84 %. This implies that PC-1 is related to a spectral feature common for all bands regardless of characteristics of observed grounds and can be attributed to reflectance or albedo of observed grounds. Therefore, PC1 is unsuitable for one of the three principal components for the purpose of spectral characterization of grounds.

The 2nd order principal component (PC2) indicates high negative values in eigenvector for Bands 5 and 7 of SWIR region and high positive values for the rest of bands of VNIR region. A number of clay minerals and carbonates have their characteristic absorption spectra in the Band 7 range, while water bodies and moisture contents of vegetation and soils show relatively low reflectance in the Band 5 range.

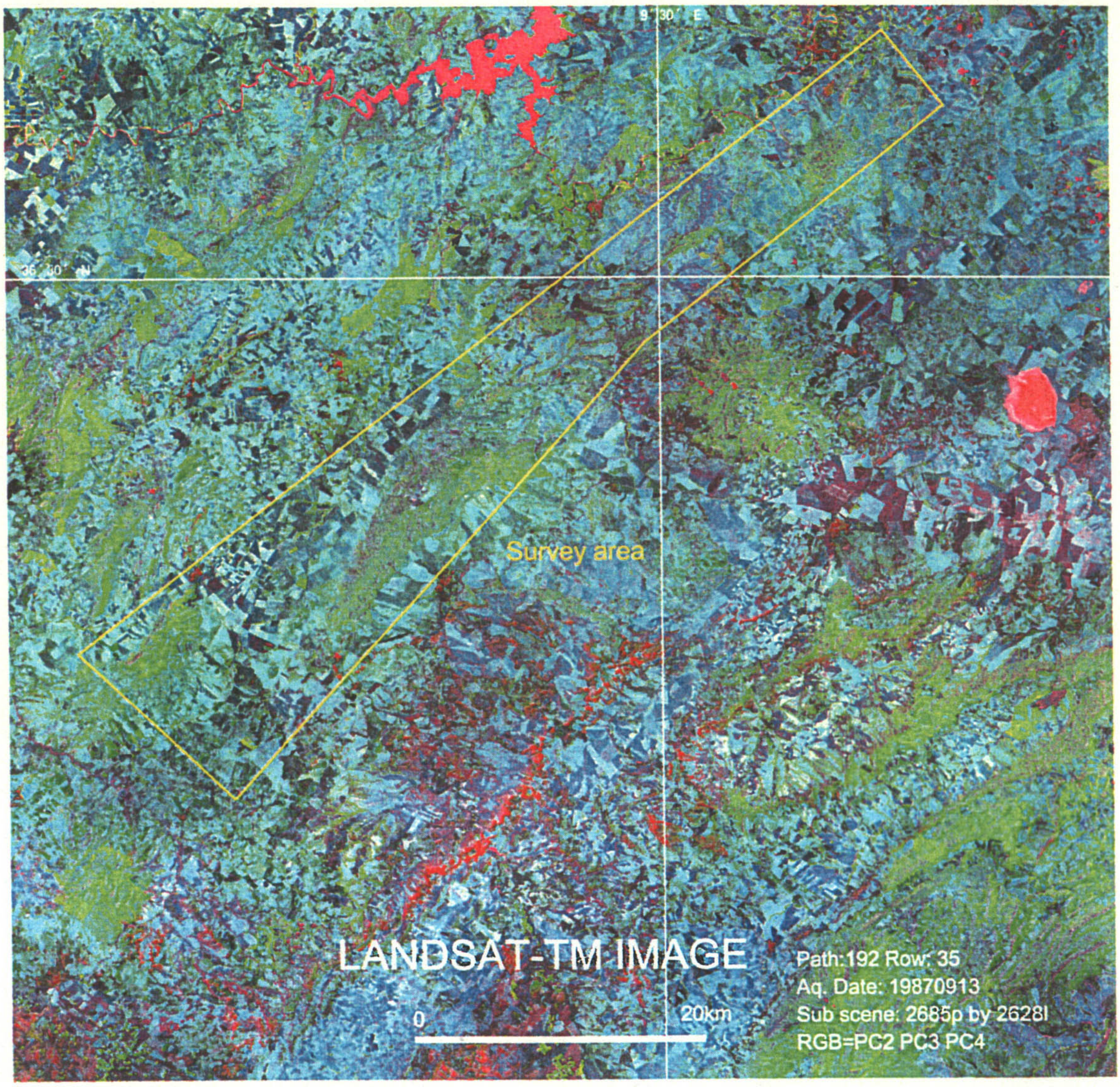

Figure 9　Principal component analysis image of Landsat-TM image (RGB=PC2·PC3·PC4)

Therefore, negative scores in PC2 may highlight either water bodies, wet lands, evergreens or areas of clay mineral and/or carbonate concentrations.

The 3rd order principal component (PC3) indicates high negative values in eigenvector for Bands 1 and 7, and high positive values for Band 4. As aforementioned, Mn and Fe, as well as other transition metals, show diagnostic absorption spectra in the Band 1 range. Since the eigenvector of Band 7 is also highly negative, it is expected that negative scores in PC3 may discern areas of concentrations of Fe, Mn, clay minerals and/or carbonates although water bodies or wet lands are also highlighted. The eigenvector of Band 4 is highly positive, which may be attributed to vegetation.

The 4th order principal component (PC4) indicates high negative values in eigenvector for Bands 4 and 7, and high positive values for Band 3 and 5. Negative scores in PC4 may outline either water bodies/wet lands, bare grounds or areas of clay mineral and/or carbonate concentrations.

The 5th order principal component (PC5) indicates high negative values in eigenvector for Bands 3 and 7, and high positive values for Band 1 and 5. Since vegetation displays a absorption spectrum in the Band 3 range, negative scores in PC5 may outlines vegetated areas as well as areas of clay mineral and/or carbonate concentrations.

There are distributed dolomite, gypsum and rock salt of Triassic, and limestone, sandstone and argillite of Cretaceous to Tertiary in the Project Area. Therefore, PC4 that is characterized by the highly negative eigenvector for Band 7 seems to be most effective for lithological discrimination, specifically for differentiating carbonate rocks. PC3 that includes the highly negative eigenvector for Band 1 may be also useful for outlining dolomite, hence diapir, outcrops with extensive development of Mn and Fe oxides due to weathering.

PC2, PC3 and PC4 are selected for principal-component image production in accordance with the assessment as above described and are assigned to red, green and blue respectively. The produced principal-component image is shown in Figure 6. Topographic features are depressed in the image with albedo (PC1) being removed, which enhances lithology and vegetation instead. In the image, reddish or bluish colors tend to indicate clay minerals and/or carbonates, while greenish colors generally coincide with iron oxides and vegetation.

(5) Photogeologic Interpretation of LANDSAT-TM Image

Photogeologic interpretation is made on the false color image of RGB = Bands 7, 4 and 1 that seems to best express geology, geological structures and lithology of the Project Area. Interpretation chart and the interpretation map of the geological structures are shown in Table 12 and Figure 10 respectively.

As the result of interpretation, 10 geologic units are distinguished. The

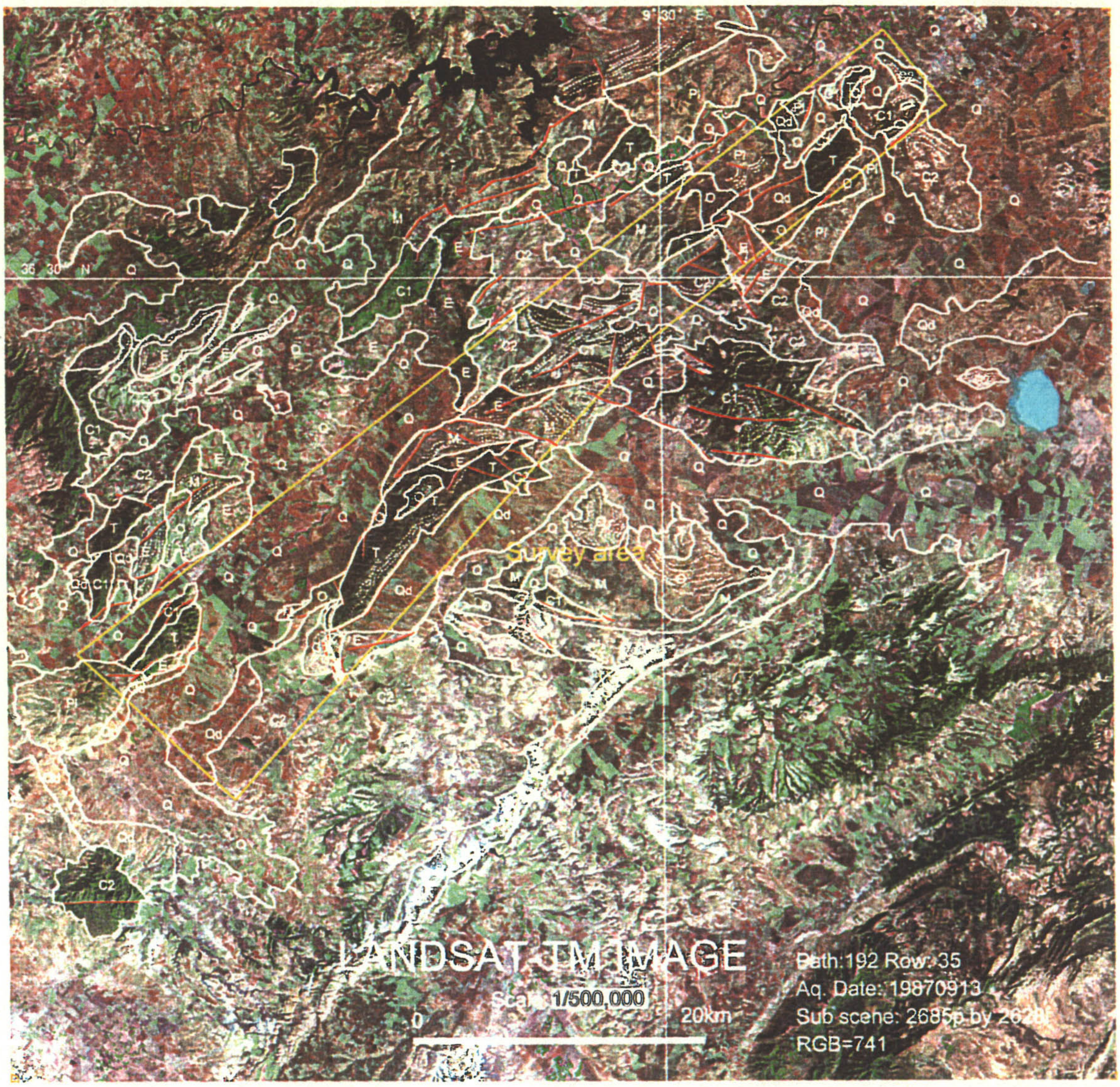

Figure 10 Interpretation map for geology of Landsat-TM image (RGB=7・4・1)

characteristics of each geologic unit are described below.

① Unit T

This unit forms dome structures elongating in the NE-SW direction in the Project Area and can be easily distinguished from other units, being dark green or dark brown in its tone and medium in its texture in the image. Beddings are also observed in part of the unit. The rocks of the unit are correlated to Triassic sediments, carbonate rocks and evapolites .

② Unit C1

This unit, comprising well bedded rocks that are resistant to erosion, varies from dark green, green, light green, dark gray to purple in its tone and is medium in its texture. These rocks are correlated to Cretaceous sediments (marl etc.) and carbonate rocks (aC2, C1).

③ Unit C2

This unit, extensively distributing in the southeastern part of the Project Area, varies from light green, purple, white to reddish brown in its tone and is fine in its texture. The rocks of the unit are moderately bedded and less resistant to erosion than those of Unit C1. They are correlated to Cretaceous sediments (marl etc., C2-E1, C2) in the geologic map.

④ Unit P

This unit, distributing in the southwestern part, varies from light green, light brown, light yellow, pink to white in its tone and is medium in its texture. The rocks of the unit are unresistant erosion. Beddings are rarely observed in association with these rocks. They are correlated ot Palaeocene sediments (Cm2-P).

⑤ Unit E

This unit varies from brown, reddish brown, green to dark brown in its tone and is fine in its texture. The rocks of the unit are unresistant to erosion, with poor development of beddings. They are correlated to Eocene sediments (E2-3, aE2-3, E1, aE-1).

⑥ Unit O

This unit is dark green, light brown or purple in its tone and medium in its texture. The rocks of the unit are moderately resistant to erosion, with poor development of beddings. They are correlated to Oligocene sediments (M1, O-M1, O, O1).

⑦ Unit M

This unit varies from light green, light brown, light yellow, pink to light gray in its tone and is medium in its texture. The rocks of the unit are moderately resistant to erosion, with moderate development of beddings. They are correlated to Miocene sediments (M3).

⑧ Unit Pl

This unit is light green, yellow or light yellow in its tone and medium in its texture. The rocks of the unit are moderately resistant to erosion, with poor development of beddings. They are correlated to Pliocene sediments (Pl, M-Pl) in the geologic map.

⑨ Unit Qd

This unit, distributing along hill-slopes, is brown or light green in its tone and very fine in its texture. It comprises Quaternary sand dunes (dQ).

⑩ Unit Q

This unit extensively distributes in plains along rivers and water courses and is utilized for crop fields. It varies from brown, pink, green, light green to purple in its tone and comprises Quaternary alluvials (aQ).

Table 12 LANDSAT-TM interpretation chart (RGB=7·4·1)

Photogeologic units	Image characteristics		Geomorphological features				Correlation with Geologic map
	Tone	Texture	Drainage pattern	Drainage Density	Rock resistance	Bedding	
Q	brown, pink, green, light green, violet	none	---	---	---	none	aQ
Qd	brown, light green	very smooth	parallel	low	very low	none	dQ
Pl	light green, yellow, light yellow	intermediate	pinnate	high	moderate	rare	Pl, M-Pl
M	light green, light brown, light yellow, pink, light grey	intermediate	dendritic	moderate	moderate	modetrate	M3
O	dark green, dark brown, violet	intermediate	dendritic	moderate	moderate	rare	M1, O-M1, O, O1
E	brown, reddish brown, green, dark brown	smooth	dendritic	low	low	rare	E2-3, aE2-3, E1, aE1
P	light green, light brown, light yellow, pink, white	intermediate	dendritic	moderate	low	rare	Cm2-P
C2	light green, violet, white, reddish brown	smooth	dendritic	moderate	low	moderate	C2-E1, C2
C1	dark green, green, light green, dark brown, violet	intermediate	dendritic	moderate	high	well	aC2, C1
T	dark green, dark brown	intermediate	dendritic	high	high	moderate	T

2.2.3 JERS-1 SAR Image Analysis

(1) Data

Specifications of JERS-1 SAR data, which are used for the image analysis, are presented in Table 13. The JERS-1, Japanese satellite sensor, has the SAR sensor which is the side-looking radar with specifications shown in Table 14.

Table 13 JERS-1 SAR Data Specifications

Sensor	Path	Raw	Date of Data-Acquisition
JERS-1 SAR	303	239	10 Sep. 1996
	303	240	10 Sep. 1996
	304	239	24 Jun 1992
	304	240	24 Jun 1992

Table 14 Specifications of JERS-1 SAR Sensor

Band	1, L band
Frequency	1275 MHz
Spatial Resolution	18 m
Swath Width	75 km
Off-Nadir Angle	35°
Polarization	HH
Orbit Altitude	568 km

(2) Image Processing

Prior to image processing, JERS-1 SAR data are pretreated for edge enhancement using the median filter comprising arrays of three-by-three pixels in order to accentuate linear features in the produced image. The data sets of four JERS-1 SAR scenes, after georectified according to the same map projection parameters as shown in Table 9, are compiled into a single data set for a mosaic by digital mosaicking. A scene comprising 5330 pixels x 5205 lines, which includes the Project Area, is framed out of the mosaic for the photogeologic interpretation.

(3) Photogeologic Interpretation of JERS-1 SAR Image

In this SAR image, eastern slopes of hills are bright, contrasting with dark opposite slopes, which is resulted from foreshortening of the image with the look direction from the eastern side. Reflection intensity is influenced by backscattering of microwave that depends on roughness of ground surface. Image becomes brighter with increasing roughness. The roughness of the Project Area is dependent mainly on vegetation and lithology. Vegetated hills present bright images, while featureless plains are dark. Vegetation is well developed along water courses, in general, which makes it easier to identify drainage patterns. Water bodies such as lakes and dams are shown in black images due to mirror reflection on their smooth surfaces with nil-backscattering.

The interpreted lineament map is shown in Figure 11. Lineaments are distinct in all the terrain of Triassic, Cretaceous and Tertiary systems. Most predominated are the lineaments in the NE-SW direction, followed by those in the NW-SE and E-W directions in the general area. It is worth to note that the lineaments in the NW-SE direction are dominated in the El Akhouat Adama, Bou Khil, Bazina Kebira and Oued Jebes prospects of the Project Area, where a number of mineral occurrences have been located.

Figure 12 is the composite of the photogeologic interpretation maps using the Landsat-TM and JERS-1 SAR images. The JERS-1 SAR image is unsuitable for discriminating lithology, in comparison with the Landsat-TM image. This is because the Landsat-TM image comprises multi-spectral bands that include various spectral information with respect to lithology. On the other hand, the JERS-1 SAR image provides only information on physiographic features such as surface roughness, drainage patterns and so forth.

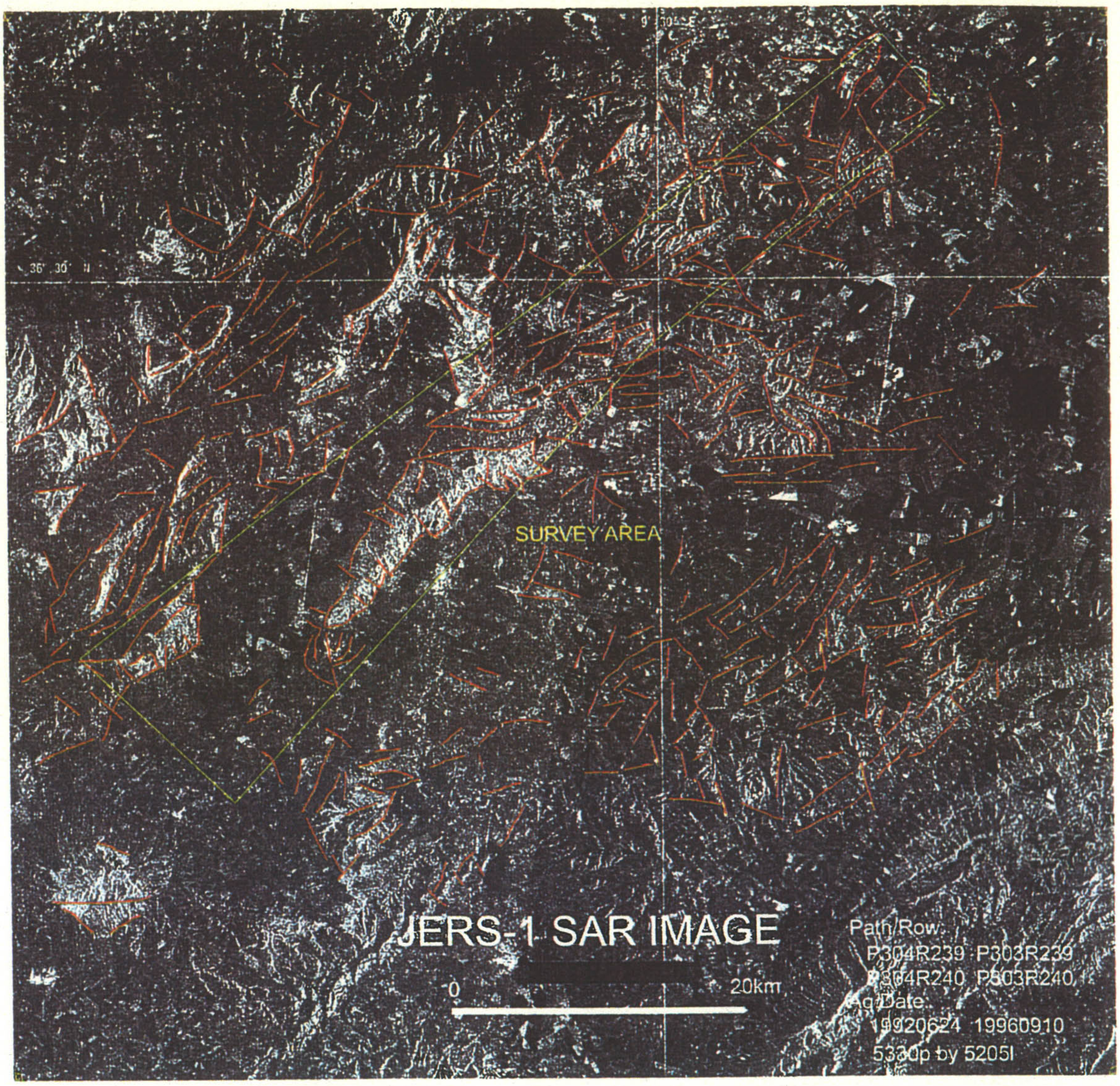

Figure 11　Lineament map of the survey area using JERS-1 SAR image

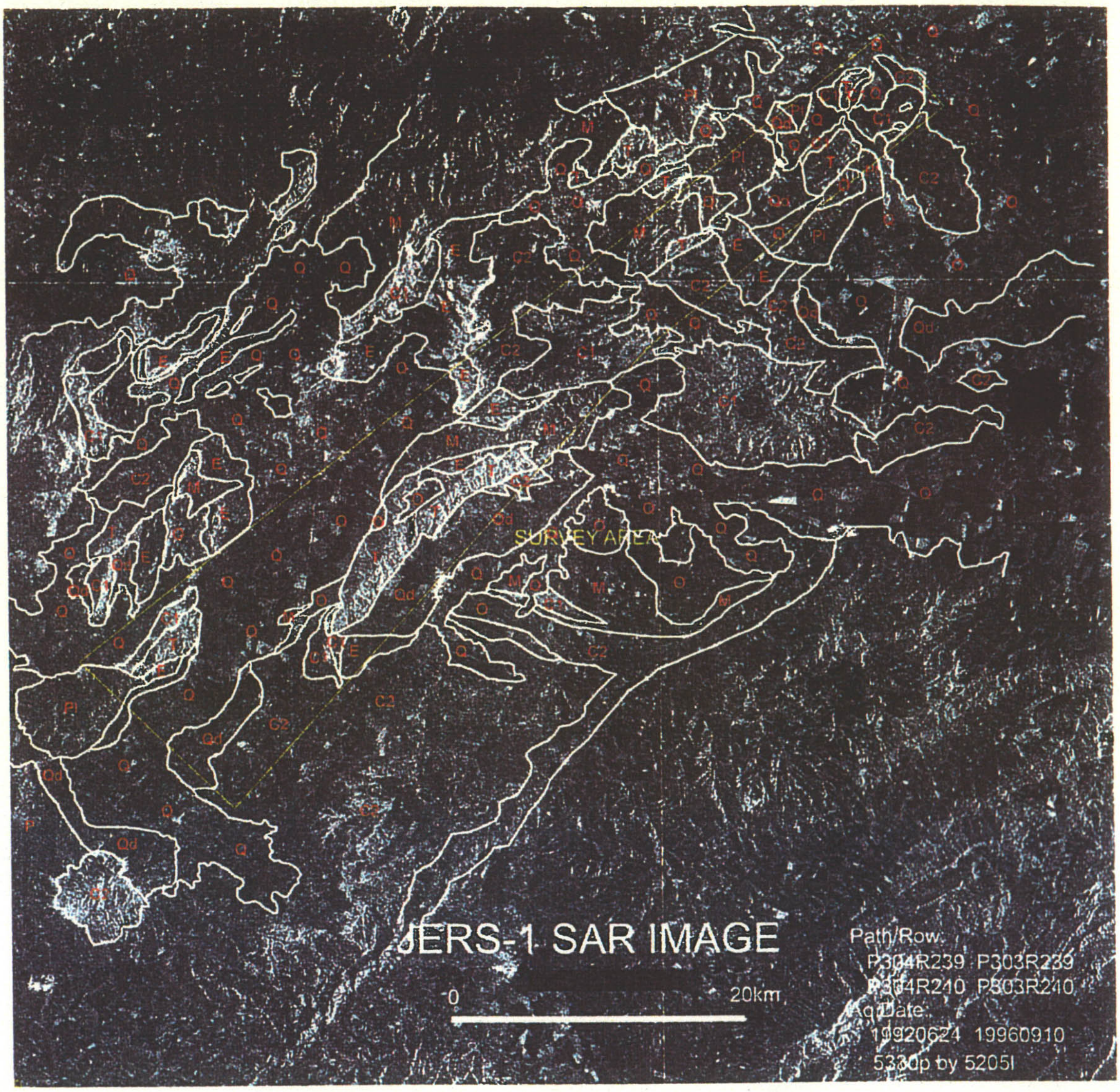

Figure 12 Retation map for geological unit